Attempt of Simple Calculation on Studying Failure Mechanism of DM Columns

B. T. T. Nguyen[1], T. Takeyama[2] and M. Kitazume[3]
[1]*Institute of Technology, Penta-Ocean Construction Co. Ltd., 1534-1, Yonkucho, Nasushiobara-shi, Tochigi 329-2746, Japan*
[2]*Department of Civil Engineering, Kobe University, 1-1 Rokkoudai, Nada-ku, Kobe, 657-8501, Japan*
[3]*Department of Civil Engineering, Tokyo Institute of Technology, 2-12-1, Ookayama, Meguro-ku, Tokyo 152-8552, Japan*
E-mail: nttbinh86@gmail.com

ABSTRACT: A simple calculation, based on limit equilibrium method, was performed to evaluate the failure pattern of deep mixing (DM) columns, used to reinforce an embankment slope. The failure modes of the columns are important in the application of DM columns, according to Japanese and the US guidelines. By using laboratory tests and numerical analysis, a certain failure mode took place with certain ground conditions, while an overall view with various modes cannot be observed. In this study, a trial of limit equilibrium method to access the failure mode of the columns is focused with an overall mechanism. As a result, while the calculation can simply predict the failure pattern of the DM columns, a parametric study was also performed to evaluate the effect of several improvement factors. Because the calculation was simplified with several assumptions, the further application of the method needs to be validated and evaluated by further studies.

KEYWORDS: Limit equilibrium method, Centrifuge model, Deep mixing, Shallow mixing, Failure pattern.

1. INTRODUCTION

Deep mixing columns have been increasingly used to support embankment, constructed on soft ground condition. Regarding the applications, the failure patterns of the deep mixing columns should be understood. The columns were reported that they may fail under high embankment pressure, with either external or internal failure patterns (Kitazume and Maruyama, 2006; 2007). In particular, in terms of the external failure, the failure causes by large deformation of the column group without any failure inside the columns while the internal failure patterns such as shearing, bending failures take place in the columns. As an example for the external failure mode of the deep mixing columns, as shown in Figure 1(a), the tilting failure of the columns, located under embankment slope, was reported by Kitazume and Maruyama (2006), using centrifuge model tests. Also, a typical failure mode of internal stability was reported with the bending pattern of the columns, as can be seen in Figure 1(b), for instance. The bending and tilting failure modes are just two examples of the failure modes, the columns may fail with various failure modes, such as shearing mode, compression/tensile mode, sliding mode, etc. (Broms, 2004). In the Japanese design guideline (PWRC, 2004), the sliding failure and circular slip failure of the deep mixing columns were currently used to check the stability of the supported embankment. While in the US, according to the Federal Highway Administration (FHWA) manual (Bruce *et al.*, 2013), the circular slip failure is also proposed to be used for designing an embankment, supported by deep mixing columns. In addition, the group of deep mixing columns should be confirmed not to fail under overturning pattern as well as bearing capacity of the bottom layer under the column group.

One of the disadvantages of the group of isolated columns is its small horizontal resistance, especially for the columns located under embankment slope. As a solution to increase the horizontal resistance of the isolated columns, the shallow mixing technique was used to construct a shallow stabilized layer to fix and reinforce the columns. Several research works were done to investigate the effectiveness of the shallow layer to reinforce the isolated columns on reducing the settlement of a high embankment(Ishikura *et al.*, 2009; Chai *et al.*, 2010) as well as on improving the slope stability (Kitazume, 2011). In previous studies, centrifuge model tests (Nguyen *et al.*, 2016a) and finite element analysis (Nguyen *et al.*, 2016b) were carried out to investigate the failure pattern of the combined structure, including the deep mixing column and the shallow layer. In terms of external stability, while the tilting failure was observed as the main failure pattern of isolated columns, the overturning failure took place significantly when using the shallow layer reinforcement. When floating-type columns were applied to support embankment, sliding failure pattern also took place together with tilting pattern or overturning one. In terms of internal stability, the bending failure was found in as a dominant failure pattern of the deep mixing columns, regardless of the reinforcement of the shallow layer.

While centrifuge model tests were performed in certain conditions, the parametric study cannot be carried out because the model test required a lot of time and effort. In addition, with a certain condition, the laboratory model test or a finite element analysis may only obtain a certain failure pattern which intends to happen with the smallest safety factor, compared amongst various failure modes. The condition of other failure modes, compared to the occurred failure mode, is still unknown. Understanding other failure modes, in an overall picture, may be helpful to evaluate the failure pattern of the columns, when varying the soil conditions as well as the improvement conditions.

For this purpose, an attempt of application of simple calculation, based on limit equilibrium method, was done in this study to evaluate the failure patterns of the deep mixing columns supporting embankment slope. The calculation was performed by using the data obtained from the centrifuge model tests. A comparison between the calculation and the model tests, on the embankment height at the failure of the supported embankment, is also addressed. Hence, the failure patterns of the deep mixing columns in the model tests and numerical analysis, with and without the shallow layer, were confirmed from the simple calculation. Together with the occurred failure mode from model tests and FEM analysis, other failure modes were also plotted for understanding the overall failure mechanism of the column. In this study, the limit equilibrium method was also used for a parametric study, to evaluate the effect of several improvement factors on the failure pattern of the deep mixing columns.

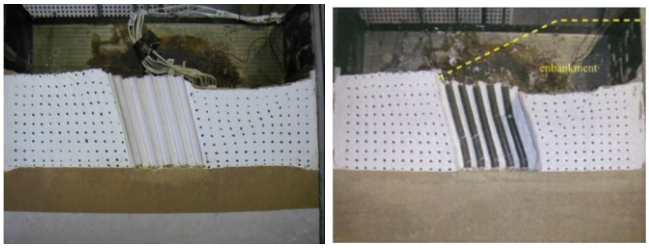

(a) Tilting failure mode (b) Bending failure mode

Figure 1 Examples of failure mode of the deep mixing columns (Kitazume and Maruyama, 2006; 2007)

2. CENTRIFUGE MODEL TESTS

2.1 Test condition

In the centrifuge tests, a model ground with a 10 m thick layer of soft clay, deposits on a 1.5 m thick sand layer, as shown in Figure 2 (Nguyen *et al.*, 2016a). A bisymmetric embankment was constructed on the clay layer at the right-hand side of the model ground. Deep mixing columns, 1 m in diameter, were used to support the embankment slope where the improvement-area ratio was confirmed about 23 %. A stabilized layer, 2 m in thickness, made by shallow mixing method, was also applied to reinforce the deep mixing columns at their tops. Nine centrifuge tests were performed as shown in Table 1 by varying the strength of the columns and the use of shallow layer. In preparation, the model columns were made in advance and curing for at least 100 days before the tests. The model ground was made by consolidating the Kaolin mixture at 1*g* condition. After consolidation, the holes were excavated by a small auger at projected positions for inserting the model columns. The shallow layer was then casted and cured inside the model container for 14 days before executing the centrifuge tests. Zircon sand with unit weight of 33 kN/m^3 was used as the embankment material.

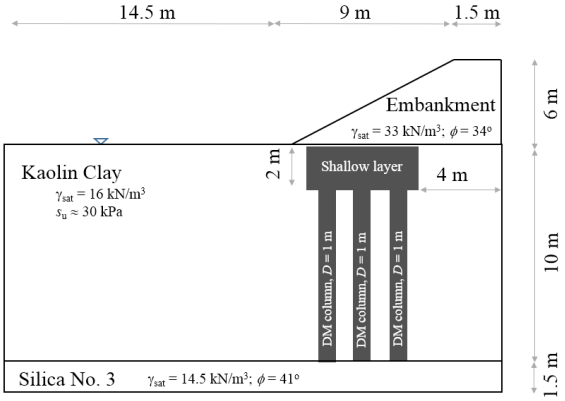

Figure 2 Centrifuge model tests (prototype scale)

2.2 Test results

2.2.1 External failure modes

Regarding external stability of the improved area, including the columns and the shallow layer, the failure patterns are shown in Figure 3 for Case 1, 2, 3 and 4. These tests were conducted with fixed-type and floating-type columns to consider the effect of the bottom layer, beneath the column group. The fixed-type condition was considered when the column bottom rested on the stiff sand layer. A thin layer of Kaolin clay (about 0.25 m in prototype dimension) was remained under the column bottom to simulate the floating-type condition. In both two different bottom conditions, the column length was kept the same. The columns experienced a tilting failure, regardless of the bottom condition as shown in Figures 3(a) and 3(b). However, in Figure 3(b), the sliding failure occurred together with the tilting one as a combination of failure patterns, when the floating-type columns were applied. In addition, the overturning failure was observed as the major pattern, in Figure 3(c), when the fixed-type columns were reinforced by shallow layer with an assumed rigid connection. A combination of overturning and sliding failures was found, in the test with floating-type columns and the shallow layer (Figure 3(d)). Similar to the isolated columns, the floating-type condition also encourages the sliding failure of the improved area. The tilting failure of the isolated columns was also reported by Kitazume and Maruyama (2006), while the effect of floating-type columns on the sliding failure mode was also observed in the previous study (Inagaki *et al.*, 2002).

2.2.2 Internal failure modes

In terms of internal stability, centrifuge tests were conducted with low-strength columns and shallow layer, as shown in Table 1 for Case 5, 6, 7 and 8. Regardless of the column strength, bending failure took place as the main pattern of the isolated columns, with several tensile cracks at the middle depth of the columns, as can be seen in Figures 4(a) and (b). The bending failure of the isolated column was also reported from previous studies (Inagaki *et al.*, 2002; Kitazume and Maruyama, 2007; Zheng *et al.*, 2013; Zhang *et al.*, 2014). In Figure 4(c) with the shallow layer reinforcement, tensile cracks, under bending failure, appeared at the connection between the columns and the shallow layer. While the failure mainly took place in the columns, the shallow layer experienced a clockwise overturning where a small crack was found near the rear columns. Similarly, the failure was observed at the connection in Case 6.

Additionally, in Case 9, the centrifuge test was carried out with high-strength columns, made of the acrylic pipe. The columns were reinforced by a low-strength shallow layer which was made by the soil-cement mixture. The excavated columns and shallow layer are shown in Figure 3(d) for the detailed failure of the improved area. In particular, large tilting can be found in the columns as the same to the external failure pattern of isolated columns (Figure 3(a)). A considerable failure occurred in the shallow layer near the rear column with large crack as shown in Figure 3(d). The failure of the shallow layer near the middle and front columns was also confirmed with small cracks. However, the opening cracks at the middle and front parts of the shallow layer are minor, compared to that at the rear side.

Table 1 Test conditions

Test cases	Test condition	Columns & SL materials	Columns' q_u (kPa)	SL's q_u (kPa)
Case 1	Fixed type columns - without shallow layer	Acrylic		
Case 2	Fixed type columns - with shallow layer	Acrylic		
Case 3	Floating type columns - without shallow layer	Acrylic		
Case 4	Floating type columns - with shallow layer	Acrylic		
Case 5	Fixed type columns - without shallow layer	Soil-cement	533.1	-
Case 6	Fixed type columns -with shallow layer	Soil-cement	533.1	269.7
Case 7	Fixed type columns - without shallow layer	Soil-cement	258.3	-
Case 8	Fixed type columns - with shallow layer	Soil-cement	258.3	164.1
Case 9	Fixed type columns - with shallow layer	Acrylic columns Soil-cement shallow layer		145

* q_u: unconfined compressive strength; SL: Shallow layer

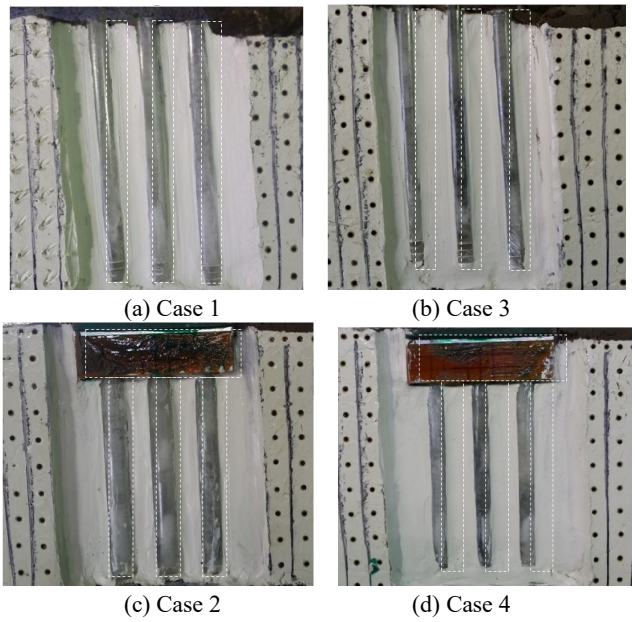

(a) Case 1 (b) Case 3

(c) Case 2 (d) Case 4

Figure 3 External stability (model tests)

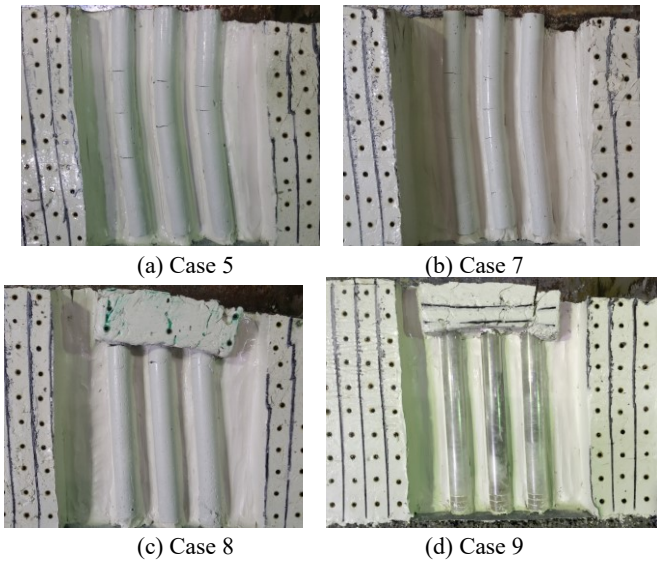

(a) Case 5 (b) Case 7

(c) Case 8 (d) Case 9

Figure 4 Internal stability (model tests)

3. SIMPLE CALCULATION

3.1 Assumed failure patterns

The failure pattern of the deep mixing columns is necessary for assessing the stability of supported embankment. According to FHWA manual, the evaluation of slope stability, together with the failure of deep-mixed structures, is strongly required in the design process while both external (global) failure and internal failure should be considered (Bruce *et al*. 2013). In the manual, slope stability should be carried out based on slip failure with various potential slip surfaces which may pass through the improved area. The improved area should also be designed sufficiently to prevent overturning failure together with bearing capacity. In addition, the current design of the Japanese guideline also proposed a simple calculation to evaluate the stability of supported embankment, based on the slip failure and the sliding failures of deep-mixed columns (PWRC, 2004). However, no clear slip failure of the embankment together with the shearing failure of the deep mixing column was observed in our laboratory experiments with the centrifuge tests. In this section, a simple calculation was proposed and conducted, based on the limit equilibrium method, adopted from the Japanese design guideline to obtain an overall picture of various failure patterns of the columns. The calculation was done by using the model ground's properties from the centrifuge experiments. Several assumptions, based on the guideline, were also required in this calculation. First, the active and passive earth pressures were assumed to follow the Rankine theory. The earth pressures were also assumed to be the same for all failure patterns, although the pressure should be dependent on the mobilization of the improved area. In the second assumption, all the columns, in each failure mode, were assumed to fail at the same time for the ease of calculation, which is different from the observation in the centrifuge model tests. The third assumption is about the stress concentration ratio, n (reported from 2 to 10), which is the ratio, between the embankment stress acting on the columns against that acting on the clay between the columns. The assumed stress concentration ratio, n of 2, was used in this calculation, after Kitazume and Maruyama (2006). By a parametric study, the stress concentration ratio shows a large effect in the sliding pattern, but negligible in others. The calculation results later show that the sliding pattern is not a dominant mode amongst other modes. The assumed n value does not much influence the discussion based on the calculation results. Further discussion will later be given in the parametric study. Finally, although the model ground in centrifuge model tests was limited by model box, the calculation was performed with the assumptions of increasing the improvement width (or the number of columns) and increasing the embankment height to achieve the failure state of the supported embankment.

3.1.1 External stability

Regarding external failure, three failure patterns, mainly observed from the centrifuge model tests, are considered in the calculation. These failure patterns include the sliding failure, the tilting failure of individual columns, and the overturning failure of the combined structure as described in Figures 5(a), (b) and (c) respectively. A safety factor of the embankment slope was considered with different failure patterns of the columns.

First, sliding failure was assumed with a horizontal movement of the improved area, together with the movement of the surrounding soil, in Figure 5(a). While all the columns were assumed to move together with the same magnitude, the same failure pattern was considered for both cases, with and without the shallow layer reinforcement. The safety factor of the supported embankment with sliding failure of deep mixing columns, based on horizontal force equilibrium, is shown in Equation (1). In the equation, the driving forces include the active earth pressures from the embankment and from the clay layer while the passive earth pressure and the shear strength, mobilizing from the bottom of the improved area, are considered as the resistances. Second, with the tilting failure in Figure 5(b), the columns are assumed to tilt around their toes individually. The safety factor is shown in Equation (2), based on moment equilibrium at the bottom of the improved area. Finally, in Figure 5(c), the overturning failure is assumed when the columns are reinforced by the shallow layer with the assumption of a rigid connection. The improved area, as a block, overturns around its front toe together with the soils inside the improved area. The safety factor of the embankment is calculated in Equation (3), based on moment equilibrium about the front toe of the column group. In this pattern, the active and passive earth pressures are assumed the same to those in the tilting failure pattern. The adhesion (M_{rc}) is only considered at the most-left and most-right columns.

$$F_s^{\text{sliding}} = \frac{P_{pc} + F_{rf} + F_{rc}}{P_{ac} + P_{ae}} \quad (1)$$

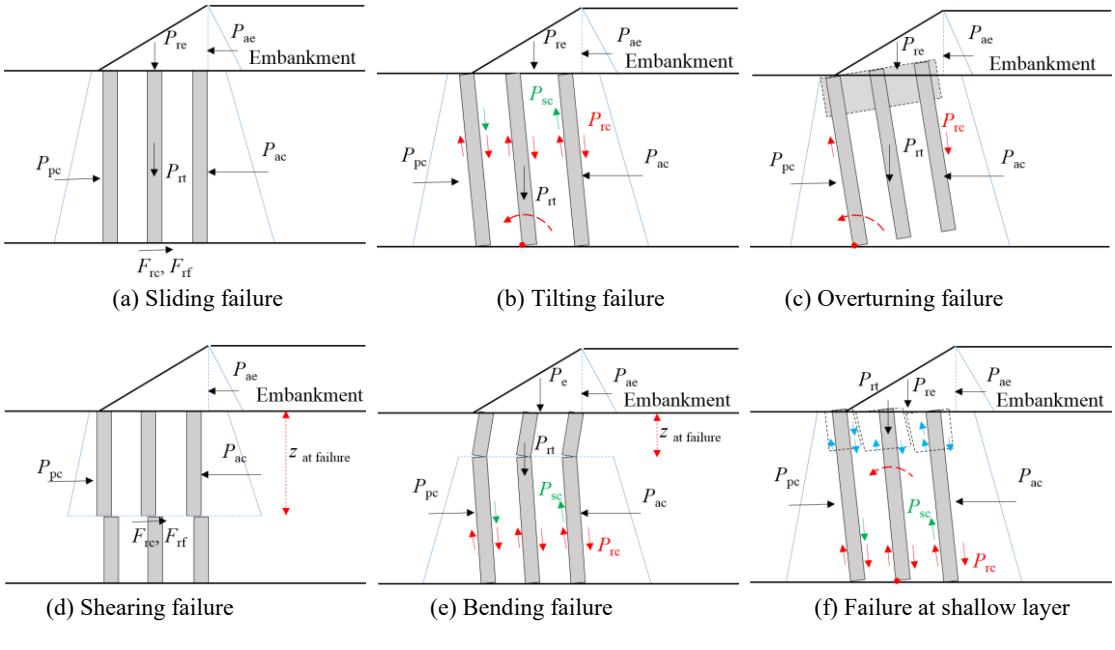

(a) Sliding failure (b) Tilting failure (c) Overturning failure

(d) Shearing failure (e) Bending failure (f) Failure at shallow layer

(g) Slip circle failure

Figure 5 Assumed failure modes of the deep mixing columns

$$F_s^{\text{tilting}} = \frac{M_{pc} + M_{rc} + M_{sc} + M_{re} + M_{rt}}{M_{ac} + M_{ae}} \quad (2)$$

3.1.2 Internal stability

By turning to the internal failure, three considered patterns, including shearing failure, bending failure in the columns, and shearing failure at the shallow layer, are described in Figures 5(d), (e), and (f) respectively. Similar to the external stability, the safety factor of the supported embankment was also considered with various failure types of the deep mixing columns.

First, as shown in Figure 5(d), the safety factor of the improved ground with the shearing failure of the columns is calculated with horizontal force equilibrium as shown in Equation (4). The failure depth ($z_{\text{at failure}}$) was obtained by computing the embankment height at failure (H_e) with various assumed failure depths. The results of the observation are shown in Figures 6(a) and (b) with various column strength (q_u) and number of columns (N). The figures show that the smallest H_e value took place at the end of the columns, regardless of the strength and the number of columns. The failure depths at the bottom of columns were assumed in shearing failure when comparing to other patterns. Second, bending failure of the deep mixing columns is considered as shown in Figure 5(e). Moment equilibrium is also assumed to calculate the safety factor of the embankment as shown in Equation (5). With an assumed failure depth, the calculation considers the column portion below the failure depth for the ease of calculation due to the negligible movement of column bottom. The lower portion of the columns is also assumed to tilt around its toe as the same to the tilting pattern. The failure depth in the bending failure was adopted from the centrifuge model tests while the bending was observed as the main pattern. In particular, in the case with isolated columns, the failure was found as the depth of 3 m from the ground surface. The test results, in the case with shallow layer reinforcement, showed the failure at the connection between the columns and the shallow layer. In the calculation, the failure depth was taken as the same the thickness of the shallow layer. While the bending strength of deep mixing columns was reported at about 10 % to 60 % of q_u (Kitazume and Terashi, 2013), the value of 28 % was assumed in this calculation (after Kitazume and Maruyama, 2007)). A parametric study also confirms a minor effect of this value on the embankment height at failure, under the bending pattern of the deep mixing columns. Finally, in Figure 5(f), the shearing failure is assumed to occur at the shallow layer while the columns experienced a tilting failure (external stability). The safety factor of the improved ground is displayed in Equation (6), the components are almost the same to those in the tilting failure pattern. The contribution of the shallow layer on the resistant moments, by the adhesion (M_{rc}) and by the shear strength of the shallow layer between the columns, is considered in this pattern.

$$F_s^{\text{overturning}} = \frac{M_{pc} + M_{rc} + M_{rt} + M_{re}}{M_{ac} + M_{ae}} \quad (3)$$

Where:

P_{ae}: total of active earth pressure of embankment (kN/m)
P_{ac}: total of active earth pressure of clay (kN/m)
P_{pc}: total of passive earth pressure of clay (kN/m)
M_{ae}: moment by active earth pressure of embankment (kN×m/m)
M_{ac}: moment by active earth pressure of clay (kN×m/m)
M_{pc}: moment by passive earth pressure of clay (kN×m/m)
M_{rc}: moment by adhesion mobilizing on the side of the column (kN×m/m)
M_{sc}: moment by shear strength of clay between the columns (kN×m/m)
M_{re}: moment by weight of embankment on the column (kN×m/m)
M_{rt}: moment by weight of the column (kN×m/m)

$$F_s^{shearing} = \frac{P_{pc} + F_{rf} + F_{rc}}{P_{ac} + P_{ae}} \quad (4)$$

Where:

F'_{rf}: total of shear strength of DM columns along failure plane (kN/m)
F_{rc}: total cohesive strength of clay (kN/m)

$$F_s^{bending} = \frac{M_{pc} + M_{rc} + M_{sc} + M_{pb}}{M_{ac} + M_{ae}} \quad (5)$$

Where:

M_{pb}: moment by bending strength and vertical load on the column (kN×m/m)

$$F_s^{SL} = \frac{M_{pc} + M_{rc} + M'_{sc} + M_{re} + M_{rt}}{M_{ac} + M_{ae}} \quad (6)$$

Where:

M_{rc}: moment by adhesion mobilizing on the side of the column (kN×m/m)
M'_{sc}: moment by shear strength of SL and clay between the columns (kN×m/m)

The slip circle failure of the supported embankment together with the improved area, as shown in Figure 5(g), is proposed in both the Japanese design guideline and the FHWA manual in the US. The slip circle failure pattern was also conducted in this study when the slip plane is assumed to cross through the improved area or through the bottom sand layer. In this pattern, a rupture breaking failure of the deep mixing columns was assumed where the shear strength of the columns was taken into account. The average shear strength of the improved area, including the deep mixing columns and the clay between the columns, was estimated by Equation (7). The Fellenius method was adapted in this calculation, where the safety factor is based on the moment equilibrium.

$$c_{u,ave} = a_s \frac{q_{u,col}}{2} + (1 - a_s) c_{u,clay} \quad (7)$$

Where:

$c_{u,ave}$: average shear strength of improved area (kPa)
a_s: improvement area ratio
$q_{u,col}$: unconfined compressive strength of DM columns (kPa)
$c_{u,clay}$: undrained shear strength of clay (kPa)

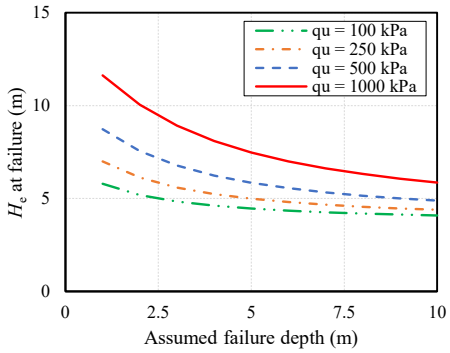

(a) Fixed-type columns

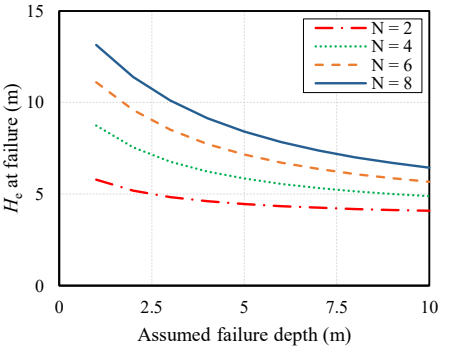

(b) Floating-type columns

Figure 6 Assumed failure depth for shearing failure

3.2 Calculation results

In the results of calculation, the embankment height at failure, H_e, which was obtained by setting the safety factor equal 1, is used for discussion on the failure pattern of the columns. It should be noted that when comparing the H_e value amongst various failure modes, the mode, with the smallest value of embankment height at failure, is assumed to happen. The calculation was conducted by using the centrifuge tests condition as well as the materials' properties.

3.2.1 External stability

The embankment heights at failure, for all three assumed patterns of the external stability, were plotted with two different bottom conditions beneath the deep mixing columns, including the fixed-type and floating-type columns. The calculation results, for the fixed-type and floating-type columns, are shown in Figures 7(a) and (b) respectively. While the embankment height at failure was plotted with various improvement widths, the results of centrifuge tests, with 4.75 m of the improvement width was also plotted for comparison. The embankment heights at the failure of the centrifuge tests were converted from the embankment pressure at yield, based on the horizontal displacement of the embankment toe.

As shown in Figure 7(a), for the fixed-type columns, the tilting failure shows the smallest value of H_e, compared to that of the sliding pattern, regarding the isolated columns. Thus, the tilting failure may take place as the main pattern of the isolated column, regardless of the improvement width. Additionally, when the shallow layer is used to reinforce the columns with the assumption of a rigid connection, the improved area is expected to work as a block. In Figure 7(a), the sliding and the overturning patterns should be considered when applying the shallow layer. As shown in the figure, the sliding pattern tends to happen with a large improvement width (more than 8 m according to the calculation), while the overturning one occurs with a small improvement width. In

comparison to the centrifuge tests, the calculation result shows a good agreement on the failure pattern of the columns with a small improvement width of 4.75 m, for the fixed-type columns. Specifically, the tilting failure took place as the main pattern of the isolated columns in the centrifuge test (Case 1 and Case 3). When using the shallow layer reinforcement, the overturning failure was dominant in the tests Case 2, that coincides with the calculated results.

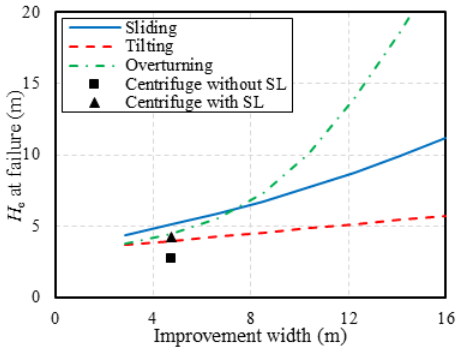

(a) Fixed-type columns

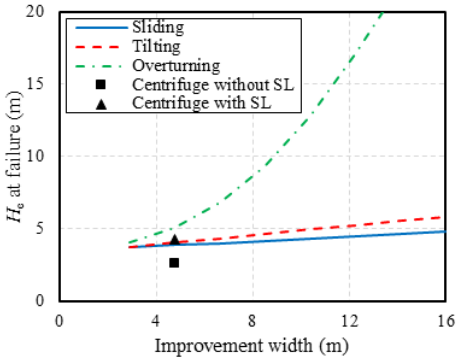

(b) Floating-type columns

Figure 7 Embankment height at failure (external stability)

By turning to the result for the floating-type columns, in Figure 7(b), the sliding failure takes place with the smallest H_e value, clearly seen at a large improvement width, irrespective of using the shallow layer. However, all three failure patterns show a similar embankment height at failure when the improvement width is about 4.75 m, as the centrifuge condition. As the same results obtained from centrifuge tests, the deep mixing columns failed with a combination of failure patterns. Specifically, the sliding and tilting failure were clearly observed in the centrifuge tests for the isolated floating-type columns (Case 2). The columns, reinforced by the shallow layer, experienced a sliding failure together with the overturning one (Case 4) which also confirms the good agreement between the observed results in the centrifuge and that in the calculation.

3.2.2 Internal stability

The calculation was conducted with the shallow layer thickness of 2 m, as the same condition in the centrifuge tests. The failure depth, in the bending pattern, was assumed at 3 m below the ground surface, to reflect the centrifuge observation. The strengths of the column and shallow layer, obtained from centrifuge tests, were also used for the calculation. The calculated results are shown in Figures 8(a) and (b), for the lower strength and higher strength of the deep mixing column. In the figure, the embankment height at failure from the centrifuge tests is also plotted. As shown in Figure 8(a), with a lower strength of the column, except the slip circle failure with a larger value of H_e, other patterns share almost the same H_e value. Hence, the failure patterns, including the bending and shearing in the columns, and the shearing at the shallow layer, may take place individually or in combination. When increasing the strength of column and shallow layer, a slightly different feature can be seen in Figure 8(b). The bending failure occurs with the smallest H_e value, especially with a large improvement width.

With a small improvement width, for instance, at 4.75 m as the centrifuge condition, the H_e values almost coincide among the bending and shearing patterns of the column as well as the shearing failure of the shallow layer. Hence, these failure patterns are possible to happen individually or in combination. In the centrifuge tests, the bending failure was observed as the dominant pattern, for both different strengths of the columns, regardless of using the shallow layer. In addition, the slip circle failure pattern did not happen in the centrifuge tests, which also agree with the calculated results.

There is a slight difference in the embankment height at failure between the centrifuge and the simple calculation, for both the internal and external stability as shown in Figure 7 and Figure 8. In the centrifuge tests, the failure pressure was assumed as the yield pressure where the failure of the model ground is about to start, while the mobilization of model ground may not fully take place at the defined failure pressure. These differences, in the assumption between the centrifuge tests and the calculation, could be the reasons for the discrepancy on the embankment height at failure between the centrifuge model tests and the simple calculation. Although the difference was found in the embankment height at failure, the failure patterns observed in the centrifuge tests were confirmed by the simple calculation not only the internal failure pattern but also the external failure one.

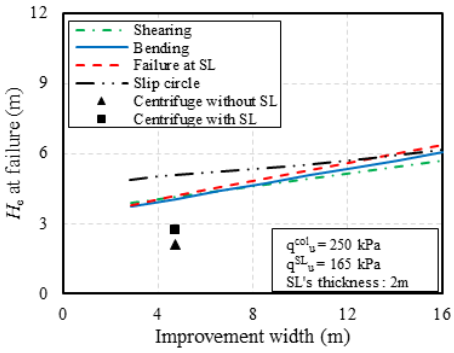

(a) Lower-strength column (q_u = 250 kPa)

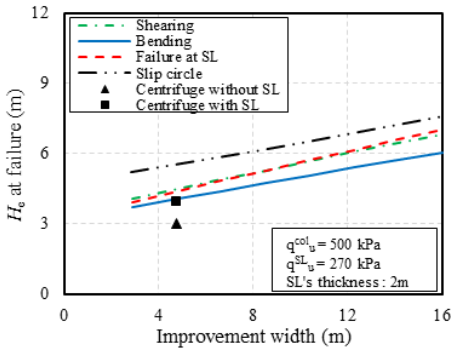

(b) Higher-strength columns (q_u = 500 kPa)

Figure 8 Embankment height at failure (internal stability)

3.2.3 Discussions

According to the calculation, for a large improvement width, the bending failure takes place as an important pattern, in terms of internal stability, regardless of the shallow layer. However, regarding the external stability, the tilting failure happens with the

isolated columns while the columns, with shallow layer reinforcement, experience a sliding failure. These observations can be obviously found with a large improvement width. With a small improvement width, tilting failure is also dominant for the isolated column while the overturning failure takes place in the columns with shallow layer reinforcement, in terms of external stability. For the internal failure of the columns, with a small improvement width, the calculation results show a possibility that various patterns may happen individually or in combination. These failure patterns include the bending and shearing failure in the columns, together with the shearing failure at the shallow layer.

As the summary of the centrifuge model tests, with a small improvement width of 4.75 m, the effect of improvement width on the failure pattern could not be observed, unfortunately. In a previous study (Nguyen *et al.*, 2016b), authors carried out numerical analyses to study the failure pattern of the deep mixing columns, using finite element method. The analysis, with the improvement width of 13 m, was also used to discuss the effect of a large improvement width on the failure pattern of the deep mixing columns. According to the FEM analysis results, the titling pattern was observed as the main failure pattern of the isolated columns, in terms of external stability. The sliding failure obviously took place in the columns, reinforced by the shallow layer. Regarding internal stability, the bending failure was considered as the significant pattern regardless of using the shallow layer. These dominant failure patterns are also observed from the calculation in the same condition with a large improvement width. By turning to the centrifuge tests, with a small improvement width, the tilting failure was also observed as an important failure pattern of the isolated column, in terms of external stability. Also, the overturning pattern clearly occurred in the columns with the shallow layer reinforcement. The observation of the external failure pattern, in centrifuge tests, coincides with that obtained from the calculation. Concerning the internal stability, while the calculation shows that various failure patterns may take place, the bending failure was observed as a dominant pattern in the centrifuge tests. It can be said that the possibility of applying simple calculation, on predicting the failure modes of the deep mixing columns, can be validated from the centrifuge and FEM analysis results.

3.3 Parametric study

A parametric study was extendedly conducted for evaluating other improvement factors which may influence the failure pattern of the deep mixing columns. Four main factors are focused in this discussion including the use of the shallow layer, the strength of columns, the spacing of columns (or improvement-area ratio) and the diameter of the column. The calculation in this parametric study was carried out with a larger improvement width until about 40 m for generally considering the effect of these factors.

3.3.1 Effect of shallow mixing layer

The calculation was conducted with the constant column strength (q_u = 500 kPa) while the column diameter of 1.5 m was applied with a center-to-center spacing of 2.8 m (or a_s of 23 %) and the stress concentration ratio, n, of 2. The results of embankment height at failure are shown in Figure 9 when the calculation with isolated columns is compared to that with columns reinforced by the shallow layer. As can be seen in Figure 9(a) for the isolated columns, irrespective of improvement width, the bending and tilting failures tend to happen with the smallest H_e value. When the columns are reinforced by the shallow layer with 2 m thickness, shown in Figure 9(b), the bending also takes place with a slight increase of the H_e value, compared to that in the isolated columns. It can be said that using the shallow layer to reinforce the isolated columns has a small effect on increasing the embankment height at the failure of the column while the bending failure is dominant in both conditions.

In addition, the effect of shallow layer thickness was also studied by increasing the thickness to 6 m, as shown in Figure 9(c). Due to the changing in the failure depth when increasing the thickness of the shallow layer, a significant increase of the H_e value with the bending failure can be found, compared to the results with 2 m thickness of the shallow layer in Figure 9(b). With thicker shallow layer, both bending and shearing failures are possible to happen with the smallest embankment height at failure.

As a summary, while the shallow layer shows a small effect on increasing the failure load of the columns, a greater effect can be achieved when increasing the thickness of the shallow layer. By looking at the effect of improvement width (or the number of columns), a significant influence on increasing the H_e value, based on the bending pattern, can be observed, even with the isolated columns or the columns reinforced by the shallow layer.

3.3.2 Effect of column strength

The calculations were conducted by changing the column strength (q_u of 500 kPa and 2000 kPa) for the isolated columns. As the results shown in Figure 10, when increasing the column strength, a significant increase of H_e value, with the shearing and the slip circle failure patterns can be found. The effect of q_u value is minor on increasing the embankment height at failure based on bending pattern. Regardless of improvement width, the bending and tilting are possible to happen with the smallest H_e value. It can be said that the effect of columns strength on the embankment height at failure is not considerable while the bending failure takes place, regardless of the column strength.

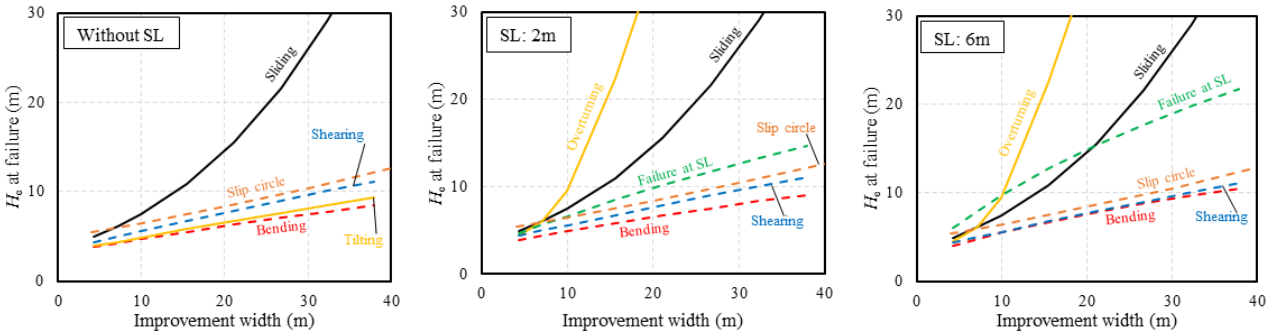

(a) Isolated columns (b) Shallow layer of 2 m thickness (c) Shallow layer of 6 m thickness

Figure 9 Effect of the shallow layer

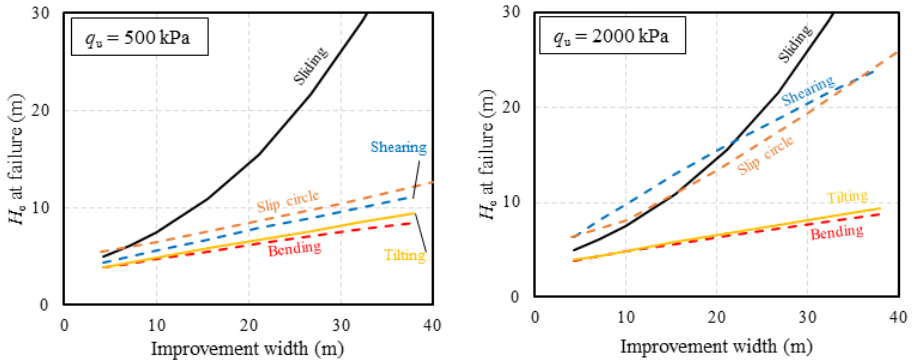

Figure 10 Effect of the strength of columns

3.3.3 Effect of improvement-area ratio

While keeping the column strength at constant (q_u = 500 kPa), the calculation was conducted by changing the column spacing with a column diameter of 1.5 m for the isolated columns. The improvement-area ratio of 23 % and 67 % were used where the results are shown in Figure 11. As shown in the figure, when increasing the a_s value, an obvious increase of the H_e value is confirmed for the bending and tilting patterns, which are the dominant failure patterns. However, the effect is not significant, compared to the strong effect on the shearing, sliding and slip circle patterns. The bending failure is observed as the main failure pattern with smallest H_e value especially with the large value of a_s. The embankment height at failure is mainly dependent on that with the bending failure. In that sense, the effect of a_s is also not significant regarding the failure load of the columns.

3.3.4 Effect of column diameter

The embankment heights at failure, for the isolated columns with different column diameters of 0.5 m, 1 m, and 1.5 m, are presented in Figure 12. While keeping the same column spacing of 2.8 m, the H_e value was calculated with the q_u value of 500 kPa. By increasing the column diameter, the H_e value of sliding failure significantly increased which is also the highest value, amongst other patterns. As shown in the figure, by changing the column diameter from 0.5 m to 1.5 m, the shearing or slip circle failure is replaced by the bending or tilting failure, with a clear increase of H_e at failure. However, the effect of column diameter on increasing embankment height at the failure of the columns is not significant in general.

3.3.5 Effect of stress concentration ratio (*n*)

The stress concentration ratio, n, is one of the key parameters to ecaluate the stability of the improved ground. The effect of stress concentration ratio, *n*, on the failure pattern was also considered by keeping the column diameter of 1.5 m, the improvement-area ratio of 23 %. The calculation was performed with different ratios of stress concentration of 2, 5, and 10 as the results are shown in Figure 13 (from the left to the right order). As can be seen in the figure, the stress concentration ratio has a considerably influence on the sliding failure. The resistance in the sliding failure is strongly dependent on the friction between the columns and the bottom sand layer which is affected by the stress concentration ratio. While the stress concentration ratio has no effect on the slip circle and the shearing failure patterns, a small effect was recorded in the bending and tilting failure ones. In term of failure pattern, based on the centrifuge model condition, the bending or tilting patterns may take place with the smallest H_e value. The sliding mode, with the largest H_e value does not happen. It means that in the considered condition, the effect of stress concentration on the failure pattern is not considerable as far as the ground condition studied.

As a summary of the parametric study, regarding the failure of the columns, the number of columns has a significant contribution to increasing the embankment load (or embankment height) at the failure while the bending failure pattern tends to happen in most of the cases. The embankment pressure at the failure of columns is dominantly dependent upon the critical pressure of bending failure pattern. The effect of column diameter (D) and column spacing is moderate on increasing embankment pressure at the failure of columns. Column strength (q_u) and the stress concentration ratio (n) have a minor influence on the embankment height at failure. In terms of using the shallow layer, the thin shallow layer shows a minor influence on the failure load of columns while the thickness of the shallow greatly affects the failure load of the columns. However, regarding the displacement of the supported embankment, the centrifuge tests confirmed the effect of the shallow layer and the column strength on reducing the displacement of supported embankment. The calculation just focused on the first failure of the columns, many failures taking place in the columns under embankment pressure were confirmed from the centrifuge results. It is expected that after experiencing the first failure, the remained portions of columns still can contribute to reducing the displacement of the embankment.

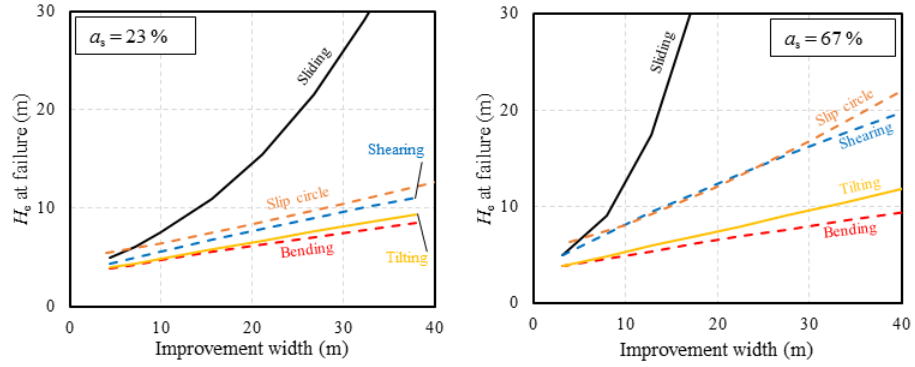

Figure 11 Effect of improvement area ratio (a_s)

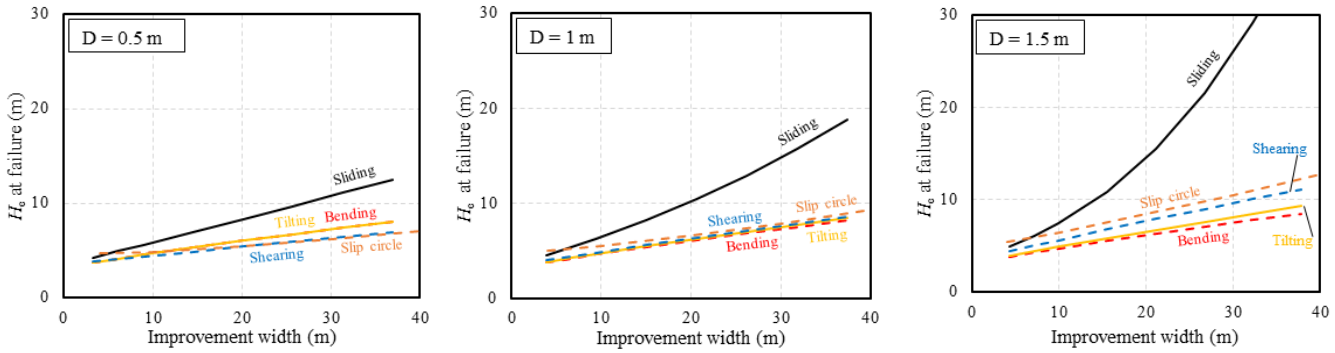

Figure 12 Effect of the diameter of columns

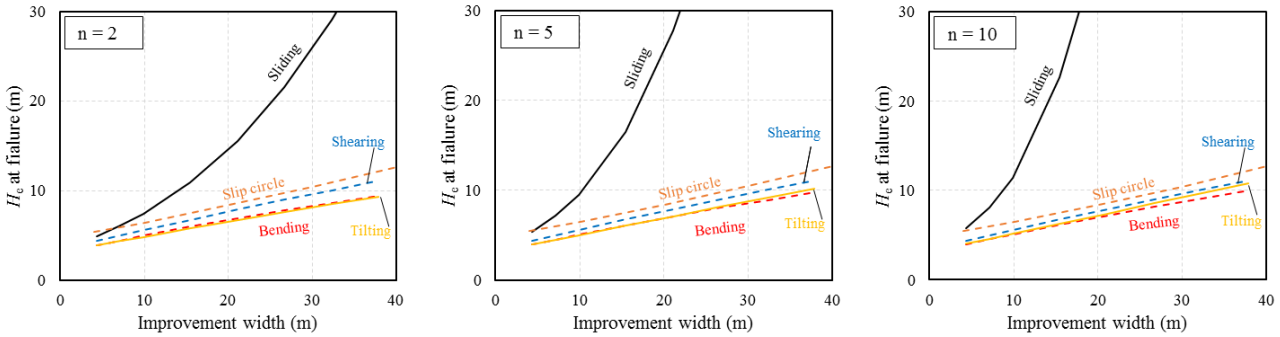

Figure 13 Effect of the stress concentration ratio

4. SUMMARY AND CONCLUSION

The study was conducted with an attempt of using limit equilibrium method to evaluate the failure pattern of the deep mixing columns, supporting embankment slope. Centrifuge model tests were performed to investigate the failure of columns in both internal and external stabilities, with a certain condition. The simple calculation, based on limit equilibrium method, can confirm the failure of deep mixing columns, obtained from the model tests when considering various failure modes in an overall viewpoint. The results of this study show a possibility of using a simple method to predict the failure pattern of deep mixing when the columns were used to support embankment slope. Both centrifuge and the calculation confirm that tilting and bending failure patterns are dominant amongst several failure modes of the isolated columns. When columns were reinforced by the shallow mixing layer, overturning and sliding failure can be considered as the main external failure patterns. With shallow layer reinforcement, the bending failure also dominantly took place in the deep mixing columns. Results of the parametric study show that the effect of the number of columns can contribute significantly to increasing the failure load of the deep mixing columns as well as the stability of the supported embankment. The effect of the diameter and the spacing of the columns is moderate while the influence of the column strength is not considerable as far as the ground condition studied. Finally, the application of shallow mixing layer also contributes to the increasing the failure load of columns especially with a great thickness of the layer. However, the calculation was firstly proposed with several assumptions for the ease of calculation. The calculation, based on the limit equilibrium method, should be validated and evaluated by further studies with laboratory tests and complex numerical analysis.

5. APPENDIX

Details of calculation for all failure patterns are provided in this section. In particular, six considered failure modes include sliding, tilting and overturning (external stability) as well as shearing, bending and failure at the shallow layer (internal stability). Detailed equations for both driving and resistant components are described for each failure mode.

Sliding failure

$$F_s^{\text{sliding}} = \frac{P_{pc} + F_{rf} + F_{rc}}{P_{ac} + P_{ae}} \tag{1}$$

$$P_{ae} = \gamma_e \tan^2\left(\frac{\pi}{4} - \frac{\phi_e}{2}\right)\frac{H_e^2}{2} \tag{1-1}$$

$$P_{ac} = (\gamma_e H_e - 2c_u)H_c + \gamma_c \frac{H_c^2}{2} \tag{1-2}$$

$$P_{pc} = \gamma_c \frac{H_c^2}{2} + 2c_u H_c \tag{1-3}$$

For high-strength bottom condition:

$$F_{rf} = \left(\gamma_{col} H_{col} + \gamma_e H_e \frac{n}{1 + (n-1)a_s}\right) a_s \tan\phi_s W \tag{1-4}$$

$$F_{rc} = (1 - a_s)Wc_u \tag{1-5}$$

For low-strength bottom condition ($F_{rf} = 0$):

$$F_{rc} = Wc_u \tag{1-6}$$

Where:

P_{ae}: total of active earth pressure of embankment (kN/m)
P_{ac}: total of active earth pressure of clay (kN/m)
P_{pc}: total of passive earth pressure of clay (kN/m)

F_{rf}: total of friction between columns and sand layer (kN/m)
F_{rc}: total cohesive strength of clay (kN/m)
a_s: improvement ratio
B: diameter of column (m)
c_u: the shear strength of clay (kPa)
H_c: thickness of clay layer (m)
H_{col}: height of columns (m)
H_e: embankment height (m)
H_{SL}: thickness of shallow layer (m)
n: stress concentration ratio
N: number of column lines
S: center to center spacing of columns (m)
W: width of improved area (m)
W_{SL}: width of shallow layer (m)
γ_c: unit weight of clay (kN/m^3)
γ_{col}: unit weight of column (kN/m^3)
γ_e: unit weight of embankment (kN/m^3)
ϕ_e: friction angle of embankment (degree)
ϕ_s: friction angle of sand layer (degree)

Tilting failure

$$F_s^{\text{tilting}} = \frac{M_{pc} + M_{rc} + M_{sc} + M_{re} + M_{rt}}{M_{ac} + M_{ae}} \tag{2}$$

$$M_{ae} = \gamma_e H_e \tan^2\left(\frac{\pi}{4} - \frac{\phi_e}{2}\right)\frac{H_e^2 + 3H_e H_c}{2} \tag{2-1}$$

$$M_{ac} = H_c^2 \frac{3\gamma_e H_e + \gamma_c H_c - 6c_u}{6} \tag{2-2}$$

$$M_{pc} = H_c^2 \frac{\gamma_c H_c + 6c_u}{6} \tag{2-3}$$

$$M_{rc} = \frac{\pi B^2}{4}\frac{N}{S} c_u H_c \tag{2-4}$$

$$M_{re} = \frac{\pi B^3}{8}\frac{N}{S}\gamma_e H_e \frac{n}{1 + (n-1)a_s} \tag{2-5}$$

$$M_{rt} = \frac{\pi B^3}{8}\gamma_{col} H_{col}\frac{N}{S} \tag{2-6}$$

$$M_{sc} = S(1 - a_s)(N-1)c_u H_c \tag{2-7}$$

Where:
M_{ae}: moment by active earth pressure of embankment (kN×m/m)
M_{ac}: moment by active earth pressure of clay (kN×m/m)
M_{pc}: moment by passive earth pressure of clay (kN×m/m)
M_{rc}: moment by adhesion mobilizing on the side of the column (kN×m/m)
M_{sc}: moment by shear strength of clay between the columns (kN×m/m)
M_{re}: moment by weight of embankment on the column (kN×m/m)
M_{rt}: moment by weight of the column (kN×m/m)

Overturning failure

$$F_s^{\text{overturning}} = \frac{M_{pc} + M_{rc} + M_{rt} + M_{re}}{M_{ac} + M_{ae}} \tag{3}$$

$$M_{rc} = \frac{B^2}{S} c_u H_c \tag{3-1}$$

$$M_{rt} = \left[\gamma_c (H_c - H_{SL})W + \gamma_{col} W_{SL} H_{SL}\right]\frac{W}{2} \tag{3-2}$$

$$M_{re} = \left(\frac{1}{2}\gamma_e H_e W_{SL}\right)\frac{2}{3}W \tag{3-3}$$

Shearing failure

$$F_s^{\text{shearing}} = \frac{P_{pc} + F_{rf} + F_{rc}}{P_{ac} + P_{ae}} \tag{4}$$

$$P_{ac} = (\gamma_e H_e - 2c_u)H_c + \gamma_c \frac{z^2}{2} \tag{4-1}$$

$$P_{pc} = \gamma_c \frac{z^2}{2} + 2c_u z \tag{4-2}$$

$$F'_{rf} = \frac{q_u^{col}}{2} a_s W \tag{4-3}$$

$$F_{rc} = (1 - a_s)W c_u \tag{4-4}$$

Where:
P_{ae}: total of active earth pressure of embankment (kN/m)
P_{ac}: total of active earth pressure of clay (kN/m)
P_{pc}: total of passive earth pressure of clay (kN/m)
F'_{rf}: total of shear strength of DM columns along failure plane (kN/m)
F_{rc}: total cohesive strength of clay (kN/m)

Bending failure

$$F_s^{\text{bending}} = \frac{M_{pc} + M_{rc} + M_{sc} + M_{pb}}{M_{ac} + M_{ae}} \tag{5}$$

$$M_{ae} = \gamma_e H_e \tan^2\left(\frac{\pi}{4} - \frac{\phi_e}{2}\right)\frac{H_e^2 + 3H_e(H_c - z)}{2} \tag{5-1}$$

$$M_{ac} = \frac{1}{2}\gamma_e H_e\left(H_c^2 - 2H_c z + z^2\right) + \frac{1}{6}\gamma_c\left(H_c^3 - 3H_c z^2 + 2z^3\right) - c_u\left(H_c^2 - 2H_c z + z^2\right) \tag{5-2}$$

$$M_{pc} = \frac{1}{6}\gamma_c\left(H_c^3 - 3H_c z^2 + 2z^3\right) + c_u\left(H_c^2 - 2H_c z + z^2\right) \tag{5-3}$$

$$M_{rc} = \frac{\pi B^2}{4}\frac{N}{S} c_u (H_c - z) \tag{5-4}$$

$$M_{sc} = S(1 - a_s)(N-1)c_u (H_c - z) \tag{5-5}$$

$$M_{pb} = \frac{\pi B^3}{32}\frac{N}{S}\left(\sigma_b + \gamma_e H_e \frac{n}{1 + (n-1)a_s} + \gamma_{col} z\right) \tag{5-6}$$

Where:
M_{pb}: moment by bending strength and vertical load on the column (kN×m/m)

Failure at shallow layer

$$F_s = \frac{M_{pc} + M_{rc} + M'_{sc} + M_{re} + M_{rt}}{M_{ac} + M_{ae}} \quad (6)$$

$$M_{rc} = \frac{\pi B^2}{4}\frac{N}{S}[c_u(H_c - H_{SL}) + \frac{q_u}{2}H_{SL} \quad (6\text{-}1)$$

$$M'_{sc} = S(1-a_s)(N-1)c_u H_c - c_u H_{SL} + \frac{q_u^{SL}}{2}H_{SL} \quad (6\text{-}2)$$

Where:

M_{rc}: moment by adhesion mobilizing on the side of the column (kN×m/m)

M'_{sc}: moment by shear strength of SL and clay between the columns (kN×m/m)

6. REFERENCES

Broms, B.B., (2004) Lime and lime/cement columns. In M. P. Moseley and K. Kirsch, eds. Ground Improvement 2nd edition. London and New York: Spon press, p. 431.

Bruce, C.; Collin J.; Berg, R.; Filz, G.; Terashi, M.; and Yang, D., (2013) Federal Highway Administration Design Manual: Deep mixing for embankment and foundation support, October 2013 - FHWA-HRT-13-046.

Chai, J.; Hino, T.; Kirekawa, T.; and Miura, N., (2010) "Settlement prediction for soft ground improved by columns", Proceedings of the ICE - Ground Improvement, 163(2), pp.109–119.

Inagaki, M.; Abe, T.; Yamamoto, M.; Yanagawa, Y.; Nozu, M.; and Li, L., (2002) "Behavior of cement deep mixing columns under road embankment". International Conference on Physical Modelling in Geotechnics. pp. 967–972.

Ishikura, R.; Ochiai, H.; Omine, K.; Yasufuku, N.; Matsuda, H.; and Matsui, H., (2009) "Evaluation of the settlement of in-situ improved ground using shallow stabilization and floating-type cement-treated columns". Doboku Gakkai Ronbunshuu C, 65(3), pp.745–755.

Kitazume, M., (2011) "Effect of surface improvement layer on internal stability of group type deep mixing improved ground under embankment loading", p.20.

Kitazume, M. and Maruyama, K., (2006) "External stability of group column type deep mixing im-proved ground under embankment loading", Soils and Foundations, 46(3), pp.323–340.

Kitazume, M. and Maruyama, K., (2007) "Internal stability of group column type deep mixing improved ground under embankment loading", Soils and Foundations, 47(3), pp.437–455.

Nguyen, B.; Takeyama, T.; and Kitazume, M., (2016a) "External failure of deep mixing columns reinforced by a shallow layer beneath an embankment", Journal of JSCE, 4(1), pp.92–105.

Nguyen, B.; Takeyama, T.; and Kitazume, M., (2016b) "Numerical analyses on the failure of deep mixing columns reinforced by a shallow mixing layer", Japanese Geotechnical Society Special Publication, 2(63), pp.2144–2148.

PWRC, (2004) Technical manual on deep mixing method for on land works, 334p. (In Japanese)

Zhang, Z.; Han, J.; and Ye, G., (2014) "Numerical analysis of failure modes of deep mixed column-supported embankments on soft soils", Ground Improvement and Geosynthetics. American Society of Civil Engineers, pp. 78–87.

Zheng, G.; Diao, Y.; Li, S.; and Han, J., (2013) "Stability failure modes of rigid column-supported embankments", Geo-Congress 2013. American Society of Civil Engineers, pp. 1814–1817.